Cell Reports, Volume *43*

Supplemental information

G-protein-coupled receptor 84 regulates acute inflammation in normal and diabetic skin wounds

Paula O. Cooper, Sarah S. Kleb, Satish K. Noonepalle, Veronica M. Amuso, Rohan Varshney, Michael C. Rudolph, Tanvir K. Dhaliwal, Darlene V. Nguyen, Miguel F. Mazumder, Najuma S. Babirye, Ruchi Gupta, Bao-Ngoc Nguyen, and Brett A. Shook

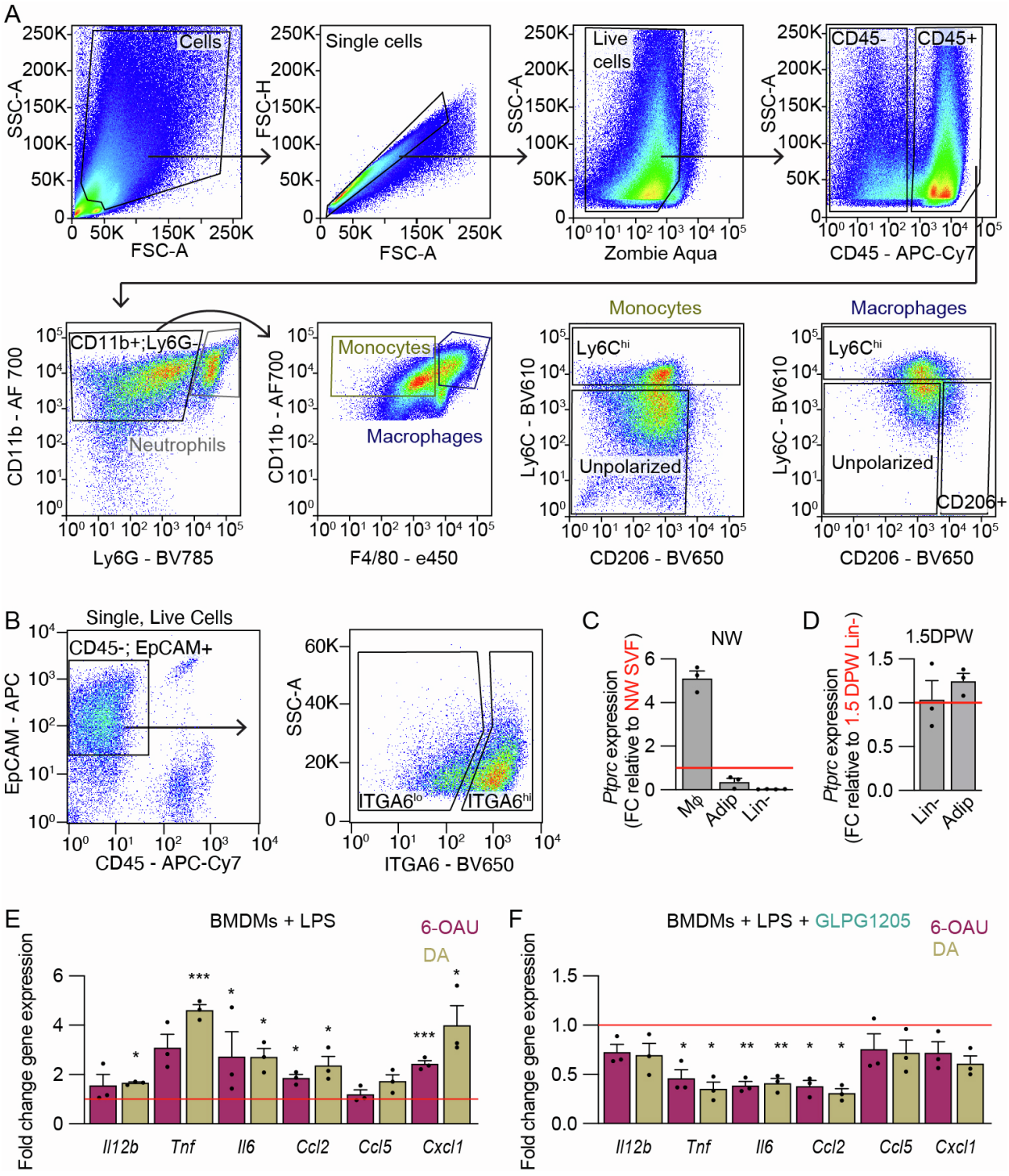
A
Cells
SSC-A
FSC-A
Single cells
FSC-H
Live cells
Zombie Aqua
CD45-
CD45+
CD45 - APC-Cy7
CD11b+;Ly6G-
Neutrophils
CD11b - AF 700
Ly6G - BV785
Monocytes
Macrophages
F4/80 - e450
Ly6C - BV610
Ly6C^hi
Unpolarized
CD206 - BV650
CD206+
B
Single, Live Cells
CD45-; EpCAM+
EpCAM - APC
ITGA6^lo
ITGA6^hi
ITGA6 - BV650
C
NW
Ptprc expression (FC relative to NW SVF)
Mφ
Adip
Lin-
D
1.5DPW
Ptprc expression (FC relative to 1.5 DPW Lin-)
E
BMDMs + LPS
6-OAU DA
Fold change gene expression
Il12b
Tnf
Il6
Ccl2
Ccl5
Cxcl1
F
BMDMs + LPS + GLPG1205

Supplemental Figure 1. Characterization of *Gpr84* expression during inflammation and pharmacological manipulation. Related to figure 1, 2, and 6. (A) Representative flow cytometry gating scheme used to assess and sort live CD45+ myeloid cell subsets and **(B)** keratinocyte populations. **(C)** Assessment of *Ptprc* expression in macrophages, adipocytes, and lineage negative (Lin-) stromal cells in NW skin. **(D)** Assessment of *Ptprc* expression in Lin- cells and adipocytes in skin 1.5 DPW ($n \geq 3$ male mice). **(E-F)** Gene expression analysis of LPS-stimulated bone marrow-derived macrophages (BMDMs) treated with **(E)** 6-OAU or DA or **(F)** GLPG1205 and 6-OAU or DA. Data are presented as the fold change relative to LPS-stimulated BMDMs (red lines) ($n = 3$ wells). Significance was determined using a two-tailed Student's t-test. Error bars indicate mean ± SEM. *$p < 0.05$, **$p < 0.01$, ***$p < 0.001$. NW, non-wounded; DPW, days post wounding; SVF, stromal vascular fraction; Mϕ, macrophage; Adip, adipocyte; Lin-, lineage negative cells; BMDM, bone marrow-derived macrophages.

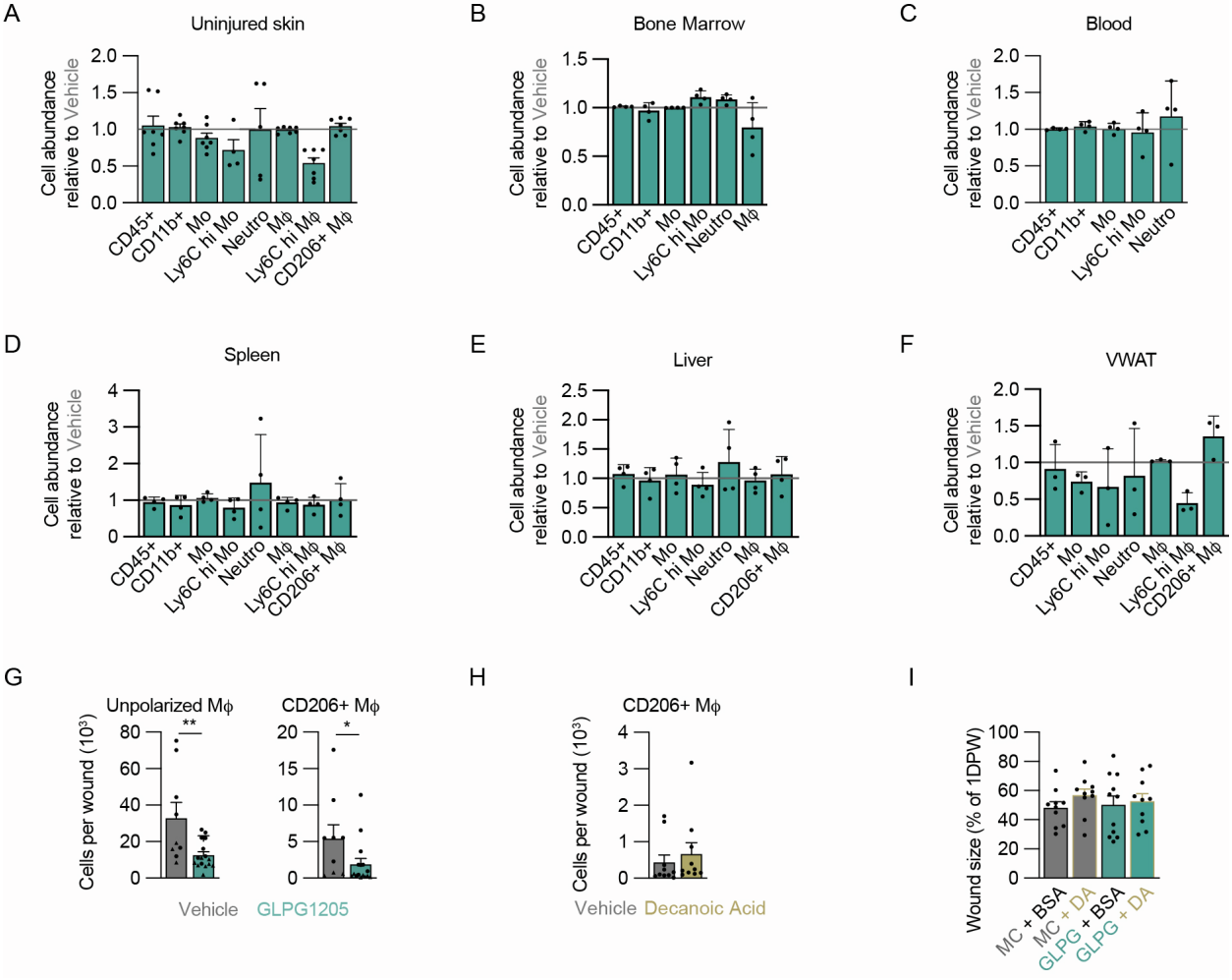

Supplemental Figure 2. Assessment of myeloid cell numbers following manipulation of GPR84. Related to Figures 1 and 2. Flow cytometry quantification of the relative abundance of immune cell subsets in **(A)** non-wounded skin, **(B)** bone marrow, **(C)** blood, **(D)** spleen, **(E)** liver, and **(F)** visceral white adipose tissue (VWAT) following 3.5 days of GLPG1205 treatment relative to vehicle-treated animals ($n \geq 4$ male mice per condition). **(G)** Quantification of macrophage subsets 2.5 DPW in vehicle- and GLPG1205-treated mice ($n \geq 9$ mice, circles denote males and triangles denote females). **(H)** Quantification of CD206+ macrophages 2 DPW in DA-treated mice compared to vehicle control ($n = 6$ male mice). **(I)** Comparison of wound size in treatment groups 2

DPW, as a percentage of their size 1 DPW (*n* = 6 male mice). Error bars indicate mean ± SEM. Significance in **(A-F)** was determined by a one-way ANOVA and in **(G-H)** by a two-tailed Student's t-test. *$p < 0.05$, **$p < 0.01$. Mϕ, macrophage; Neutro, neutrophil; Mo, monocyte; VWAT, visceral white adipose tissue; MC, methyl cellulose; BSA, bovine serum albumin.

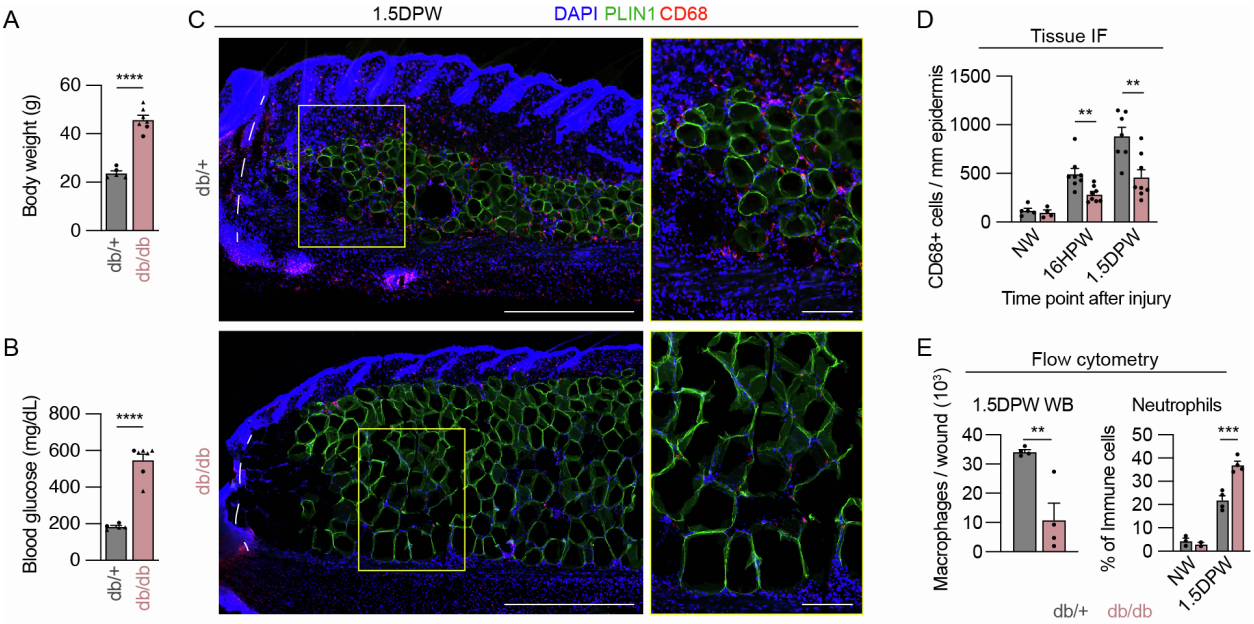

Supplemental Figure 3. Assessment of myeloid cells in diabetic mouse wounds during acute inflammation. Related to Figure 5. (A) Body weight and **(B)** blood glucose levels of db/+ and db/db mice ($n \geq 5$ mice, circles denote males and triangles denote females). **(C)** Tissue sections from 1.5 DPW wounds immunostained for Perilipin 1 (PLIN1) to delineate DWAT adipocytes and CD68 to identify macrophages. **(D)** Quantification of CD68+ cells in the dermis, including DWAT, of non-wounded skin and the wound periphery 16 HPW, and 1.5 DPW in db/+ and db/db mice, normalized to mm of overlying epidermis ($n \geq 5$ male mice). **(E)** Quantification of flow cytometry analysis of CD11b+, F4/80+ macrophages at 1.5 DPW and Ly6G+ neutrophils in NW skin and at 1.5 DPW from diabetic and lean mice ($n \geq 3$ male mice). Scale bars 500 μm in composite images and 100 μm in high-magnification images. Error bars indicate mean ± SEM. Significance was determined by a two-tailed Student's t-test. $^{**}p < 0.01$, $^{***}p < 0.001$, $^{****}p < 0.0001$. NW, non-wounded; WB, wound bed.

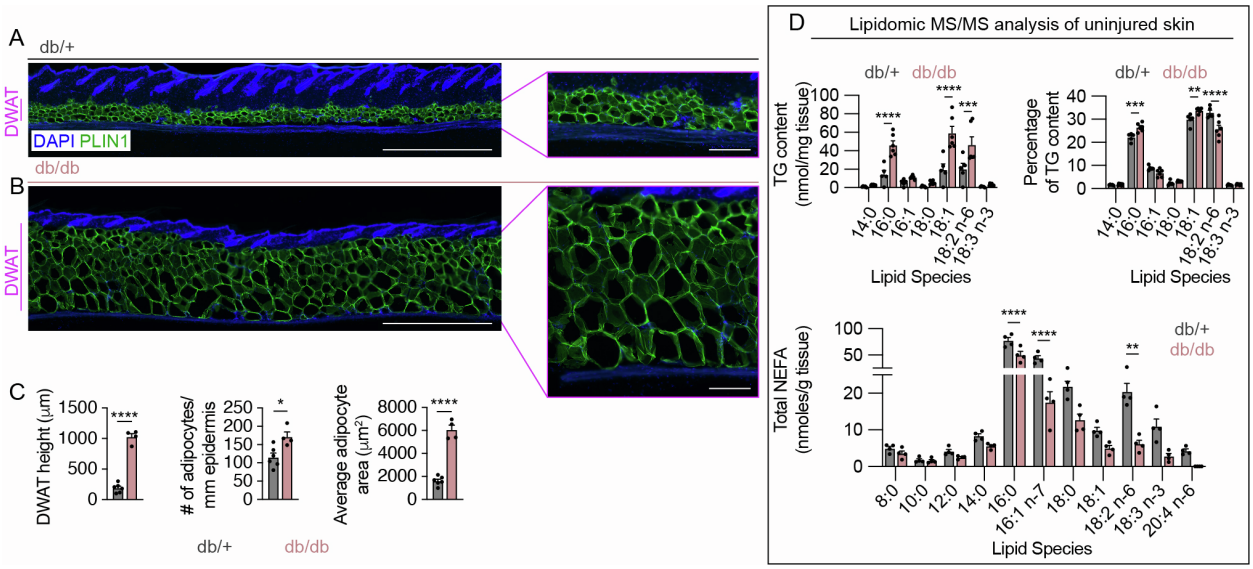

Supplemental Figure 4. Diabetes-associated changes in DWAT. Related to Figure 5. (A) Lean control (db/+) and **(B)** diabetic (db/db) skin immunostained for Perilipin 1 (PLIN1). **(C)** Quantification of db/+ and db/db DWAT height, number of adipocytes per mm of epidermis, and average adipocyte cross-sectional area (n = 4 male mice). **(D)** Lipidomic analysis of total triglyceride (TG) content, percentage of TG content, and total non-esterified fatty acids (NEFAs) in non-wounded db/+ and db/db skin ($n \geq 4$ male mice). Scale bars, 500 μm in composite images and 100 μm in high-magnification images. Error bars indicate mean ± SEM. Significance was determined by a two-tailed Student's t-test. *$p < 0.05$, **$p < 0.01$, ***$p < 0.001$, ****$p < 0.0001$. DWAT, dermal white adipose tissue.

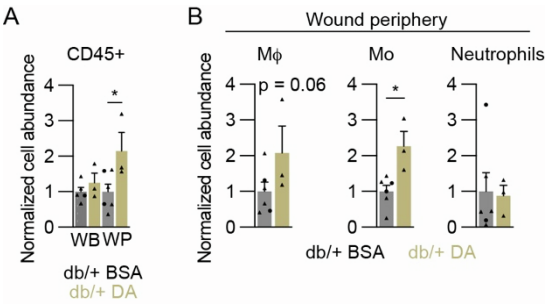

Supplemental Figure 5. Decanoic acid increases wound periphery myeloid cell numbers 2 days post-wounding in db/+ mice. Related to Figure 6. (A) CD45+ cell abundance in the wound bed (WB) and wound periphery (WP) in DA-treated db/+ mice 2 DPW, assessed by flow cytometry and normalized to BSA-treated controls. **(B)** Comparisons of macrophage (Mϕ), monocyte (Mo), and neutrophil numbers from db/+ wound periphery ($n \geq 3$ individual wounds per condition from ≥ 3 mice, circles denote males and triangles denote females). Error bars indicate mean ± SEM. Significance was determined by a two-tailed Student's t-test. *$p < 0.05$. BSA, bovine serum albumin.

Table S1: List of qPCR Primers. Related to Figures 1, 5 and S1.

Gene	Primer sequence (5'-3')	
Actb	Forward	ATCAAGATCATTGCTCCTCCTGAG
	Reverse	CTGCTTGCTGATCCACATCTG
Ccl2	Forward	GTGCTGACCCCAAGAAGGAA
	Reverse	GTGCTGAAGACCTTAGGGCA
Ccl5	Forward	TGCTCCAATCTTGCAGTCGT
	Reverse	GCAAGCAATGACAGGGAAGC
Cxcl1	Forward	TGGCTGGGATTCACCTCAAG
	Reverse	CCGTTACTTGGGGACACCTT
Il6	Forward	AGCCCACCAAGA ACGATAGTC
	Reverse	TTGTGAAGTAGGGAAGGCCG
Il12b	Forward	CGCCACACAAATGGATGCAA
	Reverse	TGTGTCCTGAGGTAGCCGTA
Gpr84	Forward	GAGTAGTGCACATGGTGGCT
	Reverse	TTCAGGATGGAGCCATACGC
Ptprc	Forward	TACGCAAAGCACGGCCTGGG
	Reverse	CTCCGGGGTTCCCACCCCTC
Tnf	Forward	AAGAGGCACTCCCCCAAAAG
	Reverse	ATCCCTTTGGGGACCGATCA